Chapter 5

Flat Flame Study : Experimental Procedure

5.1 Assembly of the Experimental Rig

The laminar flame dynamic burner described in the previous chapter was fabricated and the piping to the fuel and the air lines along with the flowmeters and the mixers were assembled. The speaker was attached to the side branch of the rig. Care was taken to ensure that there was enough spacing between the speaker mount and the side branch flange for the unhindered movement of the speaker cone. This was achieved by placing the gasketing material between the side branch flange and the speaker mounting flange.

The honeycomb with the embedded thermocouples was then fitted on the holding flange on top of the burner using high temperature silicon glue and ceramic cement. The thermocouple wires were drawn out of the side walls of the burner through a $\frac{1}{4}$" outer diameter ceramic tube having two insulated holes and attached to their respective connections. This eased the voltage measurement process. A long quartz tube was placed on the top flange of the burner so that it fitted outside the ceramic honeycomb. Fiberfrax was used to pack the gap between the tube inner diameter and the honeycomb outer diameter. It also insulated the bottom edge and the outer diameter of the quartz tube from the metallic grooved flange surface, on which the tube rested.

5.2 Assembly of the Velocity Probe

Two Radio Shack clip tie microphones were selected having the same amplitude and the same phase resonance characteristics to build a velocity probe. The frequency response characteristics of the two microphones were tested by placing them adjacent to one another in an acoustic field. The signals from the two microphones were processed using the Hewlett Packard frequency analyzer, and the frequency response function of microphone '1' with respect to microphone '2' was recorded.

Ideally, if both microphones have the same frequency response characteristics, the frequency response function should show a magnitude of zero dB (unity gain) and a phase of zero degrees. In reality, this can never be achieved, so an acceptable margin of tolerance of 0.0 $\pm$ 0.5dB in magnitude and 0.0 $\pm$ 0.5 degree in phase was set based on the accuracy range needed for proper implementation of the two-microphone technique [72]. It was ensured that for selected microphones, the frequency response function of microphone '1' with respect to microphone '2' exhibited a magnitude of 0 0 $\pm$ 0.5 dB and a phase of 0 $\pm$ 0.5 degrees. This can be verified from Figure 5.1 and Figure 5.2 which respectively show the magnitude and the phase of the frequency response function of microphone '1' with respect to microphone '2'.

The two selected microphones along with the spacing element were mounted onto a $\frac{1}{4}$" stainless steel tube using the microphone holders. The velocity sensor assembly was then inserted into the rig from the bottom through the blind flange. This enabled the probe to be moved in the axial direction and the velocity measurements could be recorded at various axial locations, upstream of the honeycomb. The probe holding tube anchored in the bottom flange was offset from the center by 13 mm, to enable the rotation of the sensor. Thus, the velocity measurements could be made at various radial locations in the plane of rotation. The microphone wires were inserted into the $\frac{1}{4}$" stainless steel tube and pulled out from the bottom, to prevent any extra flow disturbance. Outside the rig, the wires of both the microphones were soldered separately to an independent 1.5 Volt DC power source.

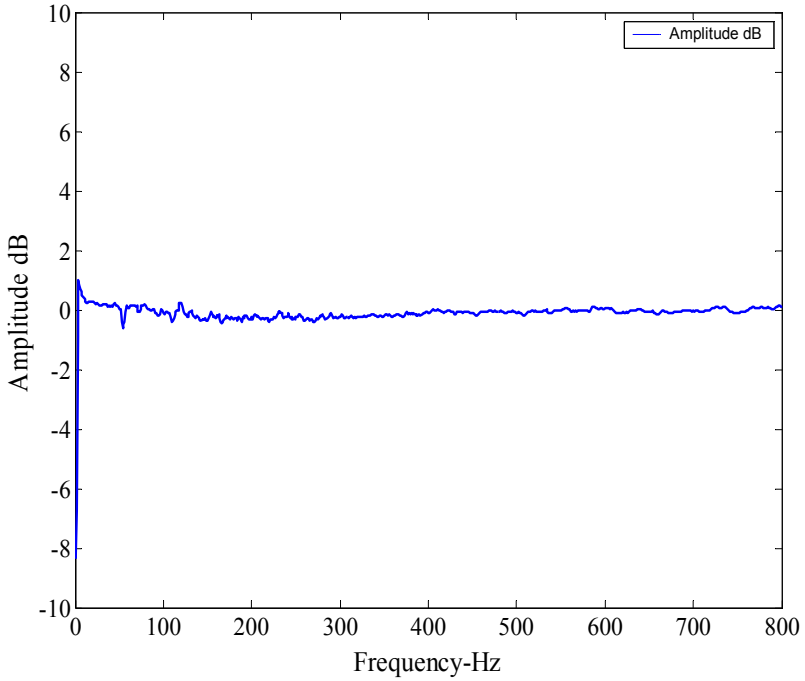

Figure 5.1: FRF (magnitude) of microphone‘1’ to microphone ‘2’

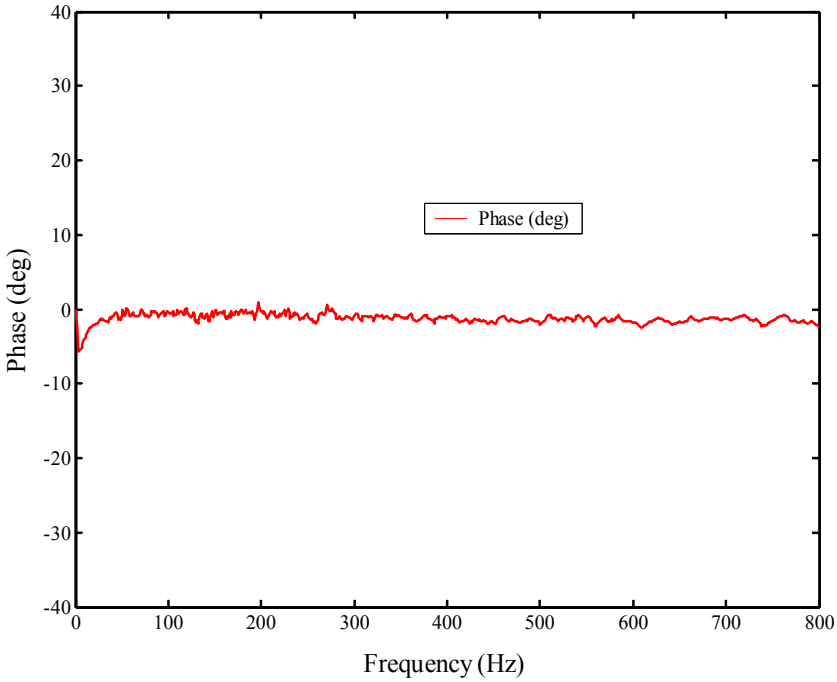

Figure 5.2: FRF (phase) of microphone‘1’ to microphone ‘2’

5.3 Acoustic Characterization

With the burner assembled, it was essential to first define the plane of the velocity measurement and characterize the rig acoustics with the measurements at this plane. To achieve an accurate transfer function of the flame response, it is essential to accurately measure the velocity perturbations hitting the flame. Therefore, the velocity measurements should be made as close to the flame as possible. Given the geometric constraints of the rig and the velocity probe, the system was assembled to obtain the velocity measurements at a plane 70 mm below the top of the flame stabilizer. This plane was established as the velocity measurement plane. The maximum temperature at the bottom face of the honeycomb was recorded to be 353K, which was well within the permissible maximum temperature limit of the microphone wire insulation nearest to the honeycomb. Thus, the plane which was 70 mm below the top surface of the honeycomb was considered for velocity measurements and was tested for its acoustic characteristics.

A 26 mm radial traverse was available due to the offset of the probe holding tube discussed in section 5.2. This corresponded to a planar circle with a diameter of 52 mm within the burner having an internal diameter of 65 mm. Using this design feature, radial velocity measurements were made at the velocity measurement plane by imparting the speaker a sinusoidal input of 0.8 volts at 344 Hz. The acoustic velocity perturbations measured at various radial locations is listed in Table 5.1. The measured velocities show that the maximum deviation from the center line velocity is about 3.9%. Thus, radially the acoustic velocity profile is reasonably flat and the one dimensional plane acoustic wave assumption is valid for the analysis of this experiment.

After validating the plane acoustic wave approximation, the velocity probe was rotated so that it measured acoustic perturbations in the center of the flow. This position of the probe was fixed and remained unchanged during the entire experiment. At this position, a frequency response function, (FRF), of the velocity probe signal and the speaker voltage, along with the coherence between the two signals was recorded, by supplying the speaker

Table 5.1: Radial acoustic velocity at a plane 70 mm below the top of the honeycomb

Radial distance from center (mm)	Acoustic Velocity x 10^3 m/sec
0	95.91
9.19	92.17
13	93.7
22.19	94.52
26	96.07

with a white noise signal from the frequency generator. The magnitude of the FRF is shown in Figure 5.3, while the coherence between the two signals is shown in Figure 5.4. The aim of this procedure was to identify the velocity modes of the burner and to identify the frequencies that generate a velocity node at the plane of measurement. From Figure 5.4, it is noted that in the frequency range of interest with respect to this experiment (i.e. 20-380 Hz), the coherence is always between 0.85 and 1, indicating that the signal from the velocity probe can be considered to be always coherent to the forced acoustic excitation. Physically, this means that the velocity probe measured accurately the fluctuating component of velocity (u') and that u' is never zero in the frequency range of 20-380 Hz, which leads to the conclusion that a velocity node does not pass through the plane of measurement between 20-380 Hz. The coherence drops rapidly after 458 Hz and is almost zero at 524 Hz. This means the velocity node occurs at the plane of measurement when the frequency of excitation is 524 Hz. The primary conclusion of the acoustic characterization is that the velocity probe provides an accurate measure of the unsteady velocity within the bandwidth of 20-380 Hz, immediately upstream of the honeycomb.

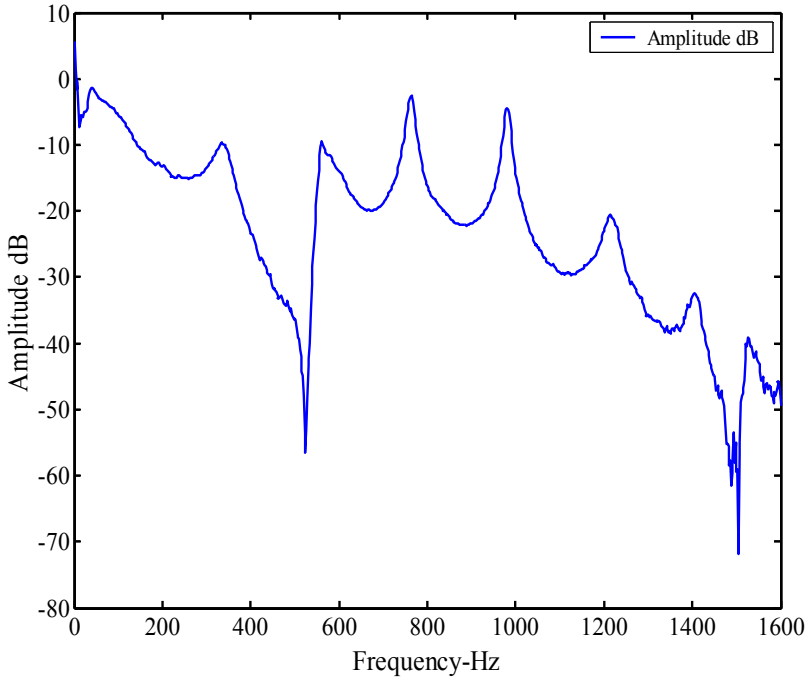

Figure 5.3: FRF of the velocity probe output and the speaker input

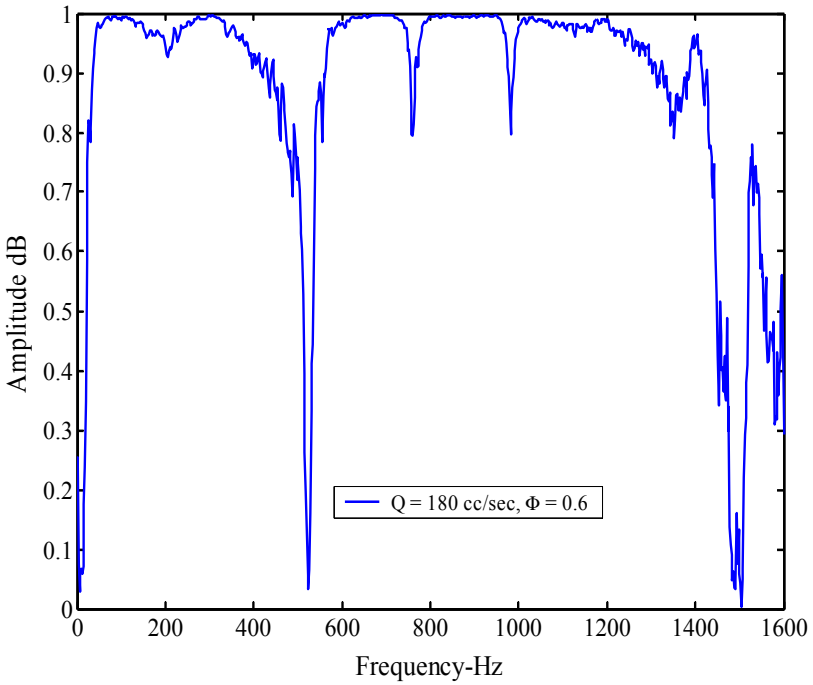

Figure 5.4: Coherence between the velocity probe output and the speaker input

5.4 Optimization of the Chemiluminescence Measurement System

Having installed the velocity probe and having the characterized the acoustics of the burner, the next step was to ensure the proper functioning of the optical system for chemiluminescence measurement. Based on the optical design described in the previous chapter, the collecting optics was mounted with a 10 mm gap kept between the two lenses, and the distance between the receiving end of fiber-optic cable and the second lens was maintained at 5 mm. The receiving optics was centered over the burner at a distance of 640 mm between the honeycomb top and the first lens, using a pair of transverse slides in radial and axial direction of the combustor. A flashlight was used to illuminate the transmitting end of the optical cable (the end attached to the monochrometer), and the image produced on the honeycomb surface was used to ensure that the optics were properly centered and focused. Finer adjustments in focusing and centering were achieved with the horizontal adjustment available on the fiber-optic cable holder. The diameter of the spot was adjusted to be 57 mm. This was achieved by changing the distance between the receiving end of fiber-optic cable and the second lens, and by moving the entire collecting optics along the vertical axis.

Having installed and adjusted the collecting optics, the free end of the fiber optic cable was attached to a beam-collimating lens that was placed in front of the inlet to the monochrometer, such that the collimated beam exiting the lens was perpendicular to the inlet slit of the monochrometer. The beam collimating lens was mounted on a three axis of freedom optical mount. The three axis of freedom were the translational and rotational movement parallel to the slit width of the monochrometer, and the rotational movement about the axis perpendicular to the slit width of the monochrometer.

The next step was to ensure that the maximum possible light transmitted through the fiber-optic cable was made incident on the diffraction grating, so that the chemiluminescence signal was maximized. This maximization of the chemiluminescent signal is achieved by ensuring that the collimated beam is perfectly perpendicular to the inlet slit of the monochrome-

ter, and both the slit widths are maintained at 900 μm. The transmission wavelength of the monochrometer was set to 3096 Angstrom, since the OH^* chemiluminescence spectrum showed a dominant peak at this wavelength.

The flame was lit and the room lights were put off to turn the room into a darkroom. The PMT power supply was then turned on. The current generated by the PMT was converted to voltage by using the current to a voltage amplifier as described in Chapter 4. The position of the collimating lens was moved by using the three axis of freedom with the aim to maximize the measured voltage from the instrumentation amplifier. Minor adjustments were made to the distance between the second lens and the fiber-optic cable inlet, and also to the orientation of the fiber-optic cable inlet. These adjustments provided a slight increase to the measured output voltage of the PMT, not because more light was captured from the flame, but primarily because of the increase in percentage of light captured from the flame that was coupled into the fiber-optic cable. Once the system was optimized, the position of the collimating lens, the collecting optics and the monochrometer was left undisturbed.

5.5 Dynamic Data Recording System

Having assembled the burners, optimized the chemiluminescent signal and acoustically characterized the rig, the last step prior to conducting the experiments was to properly hookup the dynamic data collection and flow excitation systems. The automated LABVIEW program, discussed in Chapter 4 was initiated and used for dynamic signal processing. A Hewlett Packard frequency analyzer, was used as a source for generation of sinusoidal signals that were amplified using an instrumentation amplifier, and then fed to the 8 ohm 60 watt speaker that was attached to the rig. To control the amplitude and the frequency of excitation, the communication between the Hewlett Packard frequency analyzer and the fd-daq2_lev.vi was achieved using a GPIB card. The two microphone signals were connected to the velocity probe electronics. The velocity probe output, and the OH^* signal generated by the PMT along with the voltages generated from the thermocouple were filtered by the 8 pole anti-

aliasing filters, and then fed to the National Instruments 8 channel, 16 bit simultaneous sample and hold card, SC 2040. These signals were finally processed by fd-daq2_lev.vi.

5.6 Burner Startup

Prior to running any experiment it was ensured that the collection optics were properly centered, and all electrical and electronic connections were working. The main air and fuel shut off valves were opened. The shut off valves for both the air and fuel upstream of the mixing chamber were turned on, and the metering valves were partially opened. This enabled the system to be pressurized, but no flow was allowed into the burner, as the shut off valve just upstream of the burner inlet was kept closed. The flow recording and the display program (flowDT.vi), written in LABVIEW was initialized and the flow meters were turned on. The entire flow system was then checked for leaks by applying soap water to all the tubing joints and to the entire air, fuel and premixed charge tubings. This important process was religiously carried out to maintain the accuracy of the measured flows and the safety of the working environment. To further ensure the accuracy of the flow data, the zero setting on the flow meters were periodically checked as per Hastings flow meter manual [74].

Having ensured the proper functioning of all the process control equipment, the local shut off valve just upstream of the burner inlet was turned on. The fuel and air flow rates were adjusted using their respective metering valves such that the display on the front panel of flowDT.vi program read a total flow rate of about 180 cc/sec, and an equivalence ratio, (Φ), of about 0.8. The flame was lit and was allowed to stabilize over the honeycomb for a couple of minutes. The metering valves for both air and fuel were finally adjusted to achieve the flow conditions required for the particular experiment. This initial setting was required to be readjusted in 20 minutes, as the flow meters warmed up and measured the flow more consistently. Once the final adjustment to the flow meters was made, the flame was allowed to burn and stabilize for the next 30 minutes to eliminate from the measurements slow time varying transients, such as thermal heatup of the burner. During these 30 minutes, the

room was turned into a darkroom and the power to the PMT and the current to voltage amplifier was turned on. With the monochrometer slits shut, the DC offset of the PMT output was zeroed after giving the electronics a warm up time of about 10 minutes. Once the zeroing was achieved, the monochrometer inlet slit was opened to a slit height of 15 mm. The microphones and the velocity probe circuit were turned on and were allowed to stabilize. The required corner frequency and the pre-filter and the post-filter gains were set on the anti-aliasing filter. The compensatory junctions of the three thermocouples used in the experiment were embedded in an ice bath, so as to maintain a zero degree reference for the thermocouple measurements. The contents of the water/ice bath were periodically topped off during the experimental run, to maintain the consistency and accuracy of the results.

5.7 Data Acquisition Procedure

With the confirmation that all the systems were working satisfactorily, the dynamic data acquisition process was initialized. First, the DC values of the 'Type R' and 'Type K' thermocouples were manually recorded using a voltmeter. Then using the Hewlett Packard frequency analyzer to view the chemiluminescence and the velocity signal, the speaker was forced at different frequency ranges with a sinusoidal signal and the amplitude of the forcing to achieve a linear response from the chemiluminescence and acoustic velocity signal was recorded. Linear response was defined as a condition that produced coherence between the OH^* signal and the u' signal of above 0.9 and also exhibited sinusoidal responses in the u' and OH^* signal only at the frequency of excitation. Under certain operating conditions, the above definition of the linear response was relaxed to allow the velocity power spectrum to exhibit harmonics of the excitation frequency that were at least 35 dB in magnitude lower than the magnitude at the fundamental frequency. But, under no circumstances was the OH^* power spectrum allowed to exhibit any harmonics of the excitation frequency. Once the amplitude of excitation for the various frequency ranges were determined, these were fed

into the data acquisition program fd-daq2_lev.vi. The sequence in which the fd-daq2_lev.vi stored the simultaneously collected data by the National Instruments SC2040 card could be defined on the front panel. The test panel of the data acquisition program was used to ensure all the signals were behaving correctly for an acoustic frequency at 100 Hz prior to initializing data acquisition. The program was then allowed to execute and collect the raw time traces of the various signals. The program generated a sine sweep starting with 20 Hz and at increments of 5 Hz. The last frequency for which data was collected was 380 Hz. Data was collected for 1minute at a rate of 4096 Hz. This generated enough data to perform a Fast Fourier Transform,(FFT), analysis with 30 averages over a frequency range of 0-1600 Hz, having a resolution of 0.5 Hz. Once the frequency of excitation was incremented, a 45 second wait period was given to let any transients to dissipate prior to collecting data again.

5.8 Post Processing of Experimental Data

Once an experiment was completed, the entire data set was post processed in Matlab where the frequency response function, power spectrum, and the coherence of all the signals with respect to the acoustic velocity signal were generated. The program loaded and analyzed, one at a time, the raw experimental data at each excitation frequency. After loading the time trace for a particular excitation frequency, the analysis was conducted by executing the 'spectrum' command in Matlab. For the purpose of this spectral analysis, the 'Hanning window' was used with the length of the NFFT data set fixed at 8192 data points and with no overlap. This procedure ensured that the results had a frequency resolution of 0.5 Hz and were averaged over thirty cycles.

For every excitation frequency, data was stored from all the generated power spectra, coherence and the FRF analysis at the excitation frequency and at the first harmonic. The first harmonic frequency was stored to ensure that the linear analysis criteria described earlier was satisfied. This set of reduced data for every experiment was further analyzed to obtain the order of the system, to develop reduced order models and correlate the dynamics to

physical variables. The detailed modeling procedure to obtain the reduced order models is described in Chapter 6, Section 6.2.3.